ADVANCED MATERIALS

Supporting Information

for *Adv. Mater.,* DOI: 10.1002/adma.202106728

A Ferrotoroidic Candidate with Well-Separated Spin Chains

Jun Zhang, Xiancheng Wang, Long Zhou, Guangxiu Liu, Devashibhai T. Adroja, Ivan da Silva, Franz Demmel, Dmitry Khalyavin, Jhuma Sannigrahi, Hari S. Nair, Lei Duan, Jianfa Zhao, Zheng Deng, Runze Yu, Xi Shen, Richeng Yu, Hui Zhao, Jimin Zhao, Youwen Long, Zhiwei Hu, Hong-Ji Lin, Ting-Shan Chan, Chien-Te Chen, Wei Wu*,* and Changqing Jin***

Supplementary materials

A Ferrotoroidic Candidate with Well-Separated Spin Chains

Jun Zhang†[1], Xiancheng Wang†*[1,2], Long Zhou[1], Guangxiu Liu[1,2], Devashibhai T. Adroja[3,4], Ivan da Silva[3], Franz Demmel[3], Dmitry Khalyavin[3], Jhuma Sannigrahi[3], Hari S. Nair[5], Lei Duan[1,2], Jianfa Zhao[1,2], Zheng Deng[1], Runze Yu[1], Xi Shen[1], Richeng Yu[1,2], Hui Zhao[1,2], Jimin Zhao[1,2,6], Youwen Long[1,2,6], Zhiwei Hu[7], Hong-Ji Lin[8], Ting-Shan Chan[8], Chien-Te Chen[8], Wei Wu*[9] and Changqing Jin*[1,2,6]

[1]*Beijing National Laboratory for Condensed Matter Physics, Institute of Physics, Chinese Academy of Sciences, Beijing 100190, China.*

[2] *School of Physical Sciences, University of Chinese Academy of Sciences, Beijing 100190, China.*

[3]*ISIS Facility, STFC, Rutherford Appleton Laboratory, Chilton, Oxford, OX11 0QX, UK.*

[4] *Highly Correlated Matter Research Group, Physics Department, University of Johannesburg, P.O. Box 524, Auckland Park 2006, South Africa.*

[5]*Department of Physics, 500 W. University Ave, University of Texas at El Paso, TX 79968, USA.*

[6] *Songshan Lake Materials Laboratory, Dongguan, Guangdong 523808, China.*

[7]*Max Plank Institute for Chemical Physics of Solids, Nöthnitzer Str. 40, D-01187 Dresden, Germany.*

[8]*National Synchrotron Radiation Research Center (NSRRC), 101 Hsin-Ann Road, Hsinchu 30076, Taiwan.*

[9]*Department of Physics and Astronomy and London Centre for Nanotechnology, University College London, Gower Street, London, WC1E 6BT, UK.*

† These authors contributed equally to this work

*Corresponding author: wangxiancheng@iphy.ac.cn; wei.wu@ucl.ac.uk; jin@iphy.ac.cn

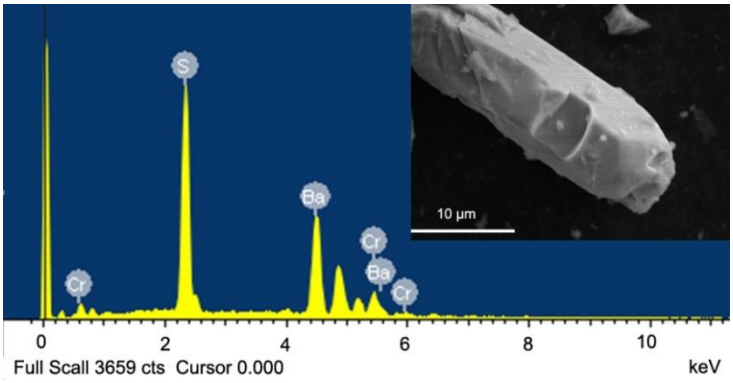

Fig. S1 The energy dispersive X-ray spectrum collected on $Ba_6Cr_2S_{10}$ single crystal. The inset shows the image of the smooth surfaces of the single crystal sample.

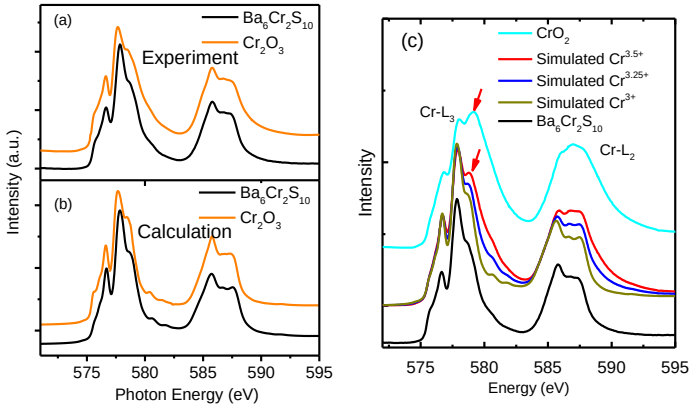

Fig.S2 (a,b) The comparison of experimental and calculated Cr-L2,3 XAS spectra of Cr_2O_3 and $Ba_6Cr_2S_{10}$. The experimental spectra for both Cr_2O_3 and $Ba_6Cr_2S_{10}$ can be well reproduced by fully intra-atomic multiplet calculations for a pure Cr^{3+} valence state including ligand field interaction. (c) The comparison of Cr-L2,3 XAS spectra of $Ba_6Cr_2S_{10}$, simulated Cr^{3+}, $Cr^{3.25+}$, $Cr^{3.5+}$ and CrO_2 with Cr^{4+}. In addition, the comparison of Cr-$L_{2,3}$ XAS of experimental $Ba_6Cr_2S_{10}$ and CrO_2 and the simulated Cr^{3+}, $Cr^{3.25+}$ and $Cr^{3.5+}$, firmly excludes the possibility of mixed valence Cr ion in our $Ba_6Cr_2S_{10}$ sample, since a clear peak occurs at ~578. 9 eV at the Cr-L_3 edge for simulated $Cr^{3.25+}$ and $Cr^{3.5+}$ and CrO_2 with Cr^{4+} against a broad weak shoulder in the experimental $Ba_6Cr_2S_{10}$ spectrum (black line).

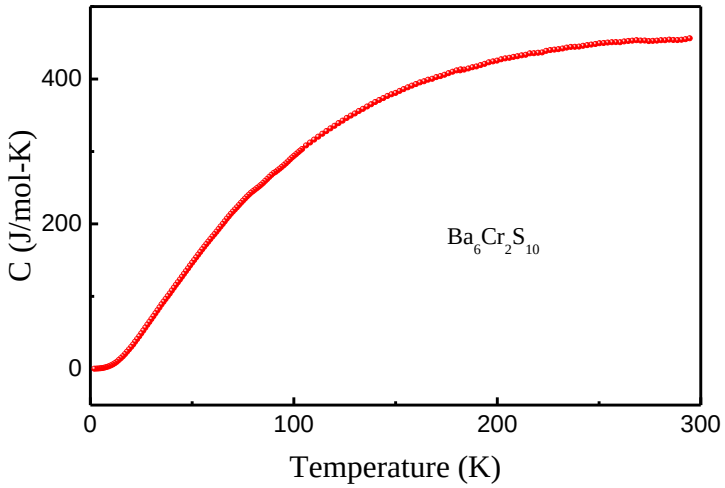

Fig. S3 The specific heat as a function of temperature between 2 K and 300 K measured at zero-field. No abnormality corresponding structural transition is observed, which suggests that the dimerized structure is kept at low temperature. Also, no λ-type abnormality can be found in the specific heat data corresponding to the magnetic transition of ~10 K.

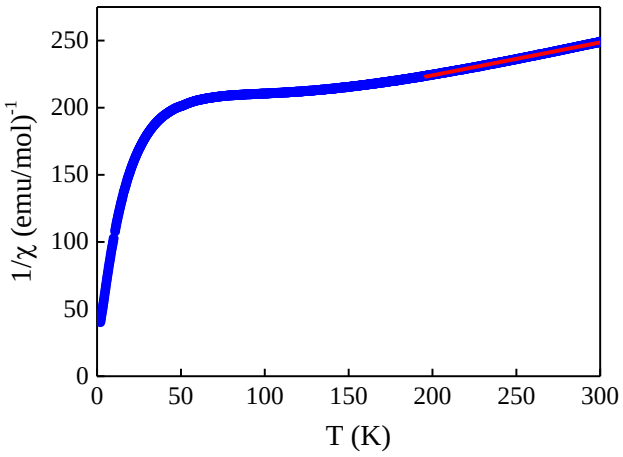

Fig. S4 The inverse of susceptibility as a function of temperature. The red line is the fit by the formula $\chi^{-1} = (T - \theta_p)/C$.

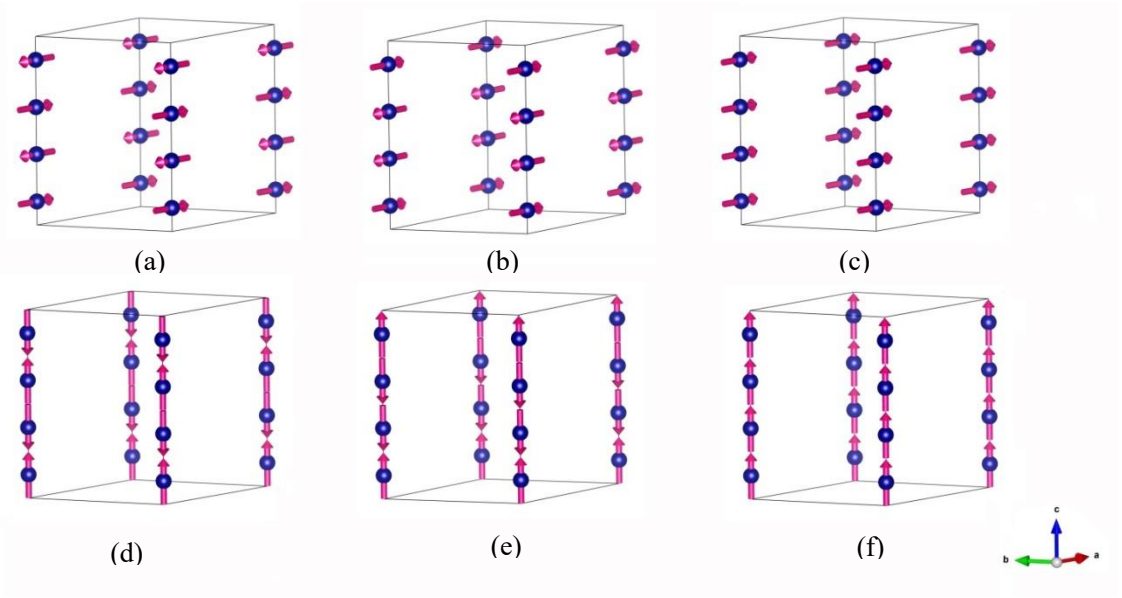

Fig. S5 Different possible magnetic structure modes for $Ba_6Cr_2S_{10}$. (a-c) The spins are oriented along the *a* axis with the spin configurations of (↑ ↓ ↑ ↓), (↑ ↓ ↓ ↑) and (↑ ↑ ↑ ↑), respectively. (d-e) The same spin configurations with that in (a-c) while the spins are oriented along the *c* axis. The models of (a-f) are labeled with *a*-AFM01, *a*-AFM02, *a*-FM, *c*-AFM01, *c*-AFM02, *c*-FM, respectively. The three modes of (a), (b) and (f) are allowed by the symmetry of the *Ama'2'* magnetic space group, but the last two modes are too small to be directly determined from the diffraction experiment.

First-principles calculations were carried out to study the electronic structure and magnetic properties of the system. The Perdew-Burke-Ernzerhof (PBE) exchange-correlation functional has been chosen[1]. The electron correlations associated with *3d* states of Cr are described by density-functional theory (DFT) + U + SOI (spin-orbit interaction) methods implemented in the Quantum Espresso code[2]. The Vanderbilt ultrasoft pseudoptentials developed for the PBE exchange-correlation functional have been chosen for all the elements throughout all the DFT + U calculations[2]. The values of U=0 and 2 eV were used for these calculations. The Monkhorst-Pack sampling of 4×4×3 has been used for all the calculations. The plane-wave cutoff energies of 544 eV and the threshold of self-consistent-field (SCF) energy convergence of 10^{-5} eV were employed throughout. A linear mix of 10% of the Fock matrix has been used to accelerate the SCF converging process.

All the energies are with reference to the *a*-AFM01 state with U=0 eV. For U=0 eV, the

energies of the structure models of (a-f) are 0 eV, 0.254 eV, 0.287 eV, 0.001 eV, 0.230 eV and 0.290 eV, respectively; while for U=2 eV, the energies of the models of (a-f) are 5.617 eV, 5.731 eV, 5.698 eV, 5.628 eV, 5.710 eV and 5.700 eV, respectively. From the calculated results, we can see that the *a*-AFM state has the lowest energy along these possible modes, which is consistent with the experimental results.

References:

[1]. J. P. Perdew, K. Burke & M. Ernzerhof, Phys. Rev. Lett. 77, 3865 (1996).

[2]. P. Giannozzi, S. Baroni, N. Bonini, M. Calandra, R. Car, C. Cavazzoni, D. Ceresoli, G. L. Chiarotti, M. Cococcioni, I. Dabo, A. Dal Corso, S. de Gironcoli, S. Fabris, G. Fratesi, R. Gebauer, U. Gerstmann, C. Gougoussis, A. Kokalj, M. Lazzeri, L. Martin-Samos, N. Marzari, F. Mauri, R. Mazzarello, S. Paolini, A. Pasquarello, L. Paulatto, C. Sbraccia, S. Scandolo, G. Sclauzero, A. P. Seitsonen, A. Smogunov, P. Umari & R. M. Wentzcovitch, J. Phys.: Condens. Matter 21, 395502 (2009).

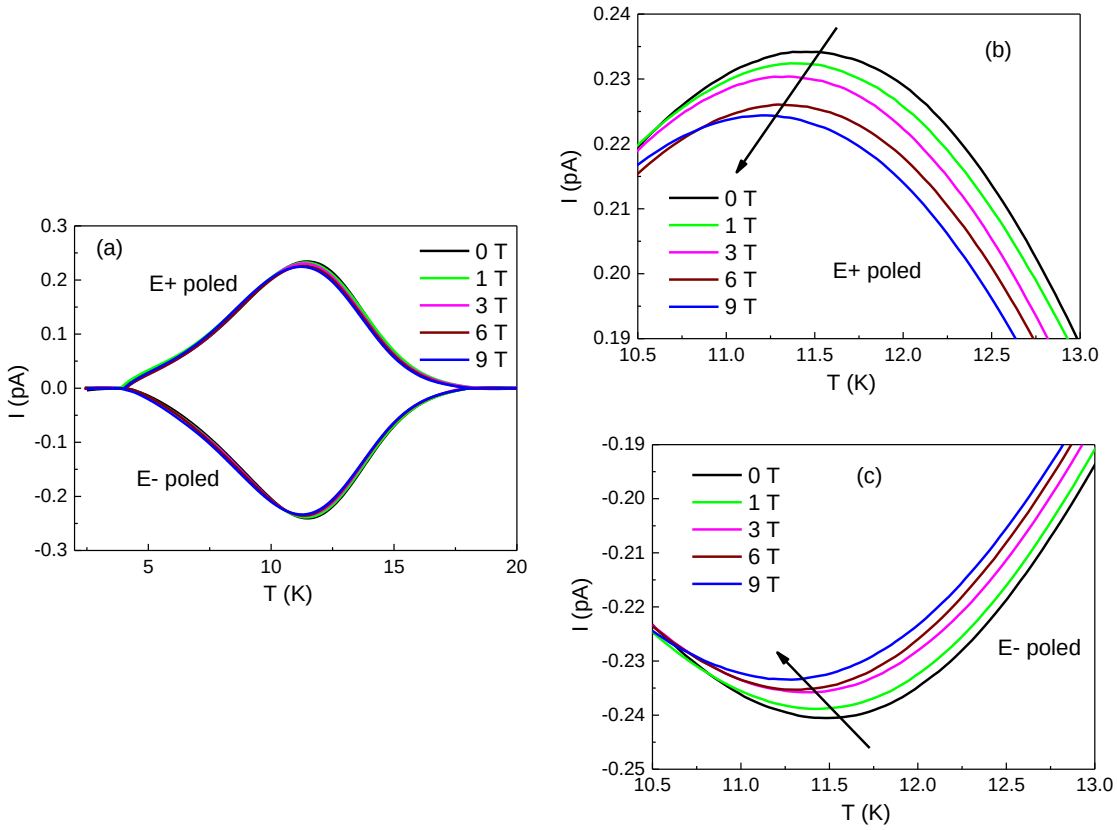

Fig. S6 (a) The pyroelectric current I_p poled from 20 K to 2 K for the polycrystalline sample of $Ba_6Cr_2S_{10}$. The enlarged view for the E+ poled (b) and the E- poled (c), showing the shift of I_p curve toward low temperature under high magnetic field.

Table S1 The positions $\vec{r}_i$ and the magnetic moment $\vec{M}_i$ of Cr cations in $Ba_6Cr_2S_{10}$. Here, the displacement ε=0.00435 and the magnetic moment S=1.03(9) μ_B, oriented along *a* axis when ignoring the canted feature. In the main manuscript, the displacement $\delta = \varepsilon \times c$ = 0.0538(4) Å. The lattice parameters are *a*=*b*=9.1228(3) Å and *c*= 12.3643(2) Å.

Site	r_i^x/a	r_i^y/b	r_i^z/c	m_i^x	m_i^y	m_i^z
Cr	0	0	7/8+ε	S	0	0
Cr	0	0	5/8-ε	S	0	0
Cr	0	0	3/8+ε	S	0	0
Cr	0	0	1/8-ε	S	0	0
Cr	1	0	7/8+ε	S	0	0
Cr	1	0	5/8-ε	S	0	0
Cr	1	0	3/8+ε	S	0	0
Cr	1	0	1/8-ε	S	0	0
Cr	1/2	√3/2	7/8+ε	S	0	0
Cr	1/2	√3/2	5/8-ε	S	0	0
Cr	1/2	√3/2	3/8+ε	S	0	0
Cr	1/2	√3/2	1/8-ε	S	0	0
Cr	-1/2	√3/2	7/8+ε	S	0	0
Cr	-1/2	√3/2	5/8-ε	S	0	0
Cr	-1/2	√3/2	3/8+ε	S	0	0
Cr	-1/2	√3/2	1/8-ε	S	0	0